Determination of Material Characteristics using Electromagnetic Forming and Weak Coupled Finite Element Simulations*

A. Brosius, M. Kleiner

Chair of Forming Technology, University of Dortmund, Germany

Abstract

The aim of this approach is to determine material characteristics of aluminium alloys (in the present case: AA5747) at very high strain rates, more precisely the relationship between yield stress, plastic strain and strain rate is figured out. To achieve high strain rates up to 10^4 s^{-1} the electromagnetic forming process (EMF) is applied, where a pulsed magnetic field is used to form materials with a high electrical conductivity during a process time between 10µs - 50µs. The advantage that EMF is a non-contact forming process can be used to determine material characteristics without any influence of friction. Additionally, in contrast to other testing methods the assumption of a mean strain rate over the process time is not needed, because the evaluation is done by finite element simulations.

To compute the associated flow curve array, where the strain rate is the third dimension, a method will be proposed combining an on-line measurement technique and iterative finite element simulations. During EMF of the tube specimen, the radial displacement of at least one significant point at the tube surface is measured on-line. These data are used as reference values for the iteration scheme. The iteration starts with the material data of a quasi-static tensile test. In order to minimise the deviations between on-line measurement and simulation result an automated data modification scheme is implemented.

The kernel of this scheme consists of an optimisation algorithm and two finite element codes. The first one is used to compute the deformation process of the specimen in a conventional transient way. The second code is implemented to calculate the body force distribution by a harmonic electromagnetic analysis. These two codes are coupled in a weak staggered approach.

Keywords:

Parameter identification, Finite Element Method, Electromagnetic Forming

---

* This work is based on the result of a research project form the DFG-SPP 1046 – The authors would like to thank the Deutsche Forschungsgemeinschaft DFG for its financial support

1 Introduction

For the description and analysis of high speed forming processes by means of finite element simulations a certain amount of knowledge about the qualitative and quantitative material behaviour during the forming process is essential. The intention of the present work is to determine yield curves at high strain rates using an iterative finite element simulation procedure. For this purpose the electromagnetic Forming (EMF) is used as a typical high speed forming process, where the energy density of a pulsed magnetic field is used for a contact less forming of metals with high electrical conductivity, such as copper or aluminium. The work-piece to be deformed will be located within the effective area of the tool coil, so that the resulting type of stress during the forming process is determined by the type of coil used and its arrangement as related to the component. Tubular components can be narrowed by means of compression coils or widened by means of expansions coils (see Figure 1).

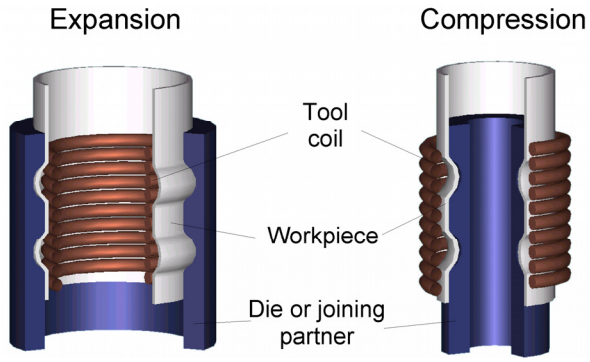

Figure 1: *Electromagnetic forming – Type of coils*

The basic idea for the determination of the dynamic material behaviour is to vary the strain rate dependent yield curves used as input for a finite element simulation (as a part from the optimisation strategy) until the calculated deformations match the measured ones. To evaluate the simulation results a comparison between the calculated radius and the experimentally determined radius is done in order to minimise the resulting difference.

In the present work the compression and expansion of a tube will be observed. At first, the important characteristics of the process serving as input for a mechanical finite element model will be determined. These will be the accurate geometrical dimensions of tool coil and work-piece, the acting body force depending on the time as well as the deformation of a significant point during the process.

2 On-line Measurement

For the comparison of experimentally obtained deformations and simulated deformations in the considered axial cross section (Figure 2a) the inner and outer contours will be measured off-line with a coordinate measurement machine (CMM) before and after the forming operation. As the geometrical data shall serve as reference values for the mechanical finite element simulation the obtained geometry at the end of the deformation is not sufficient to allow assumptions about the behaviour during the forming process. There-

fore, in addition to the off-line measurement a determination of reference data for an unambiguous description of the deformation would be useful. For this purpose an on-line measurement system based on a laser optical principle has been developed [1].

Because the forming process usually ends after a few ten microseconds, a very high time resolution had to be realised. The set-up of the developed measuring device for tube compression is shown in Figure 1a. As source of light a laser diode with line generator is used. The amount of parallel light shining through the sample is detected by a PSD (position sensitive detector) and depends on the actual inner radius of the sample. The output voltage of the PSD is proportional to the displacement of point A, in which the maximum deformation occurs. The same principle is used for the tube expansion (Figure 2b).

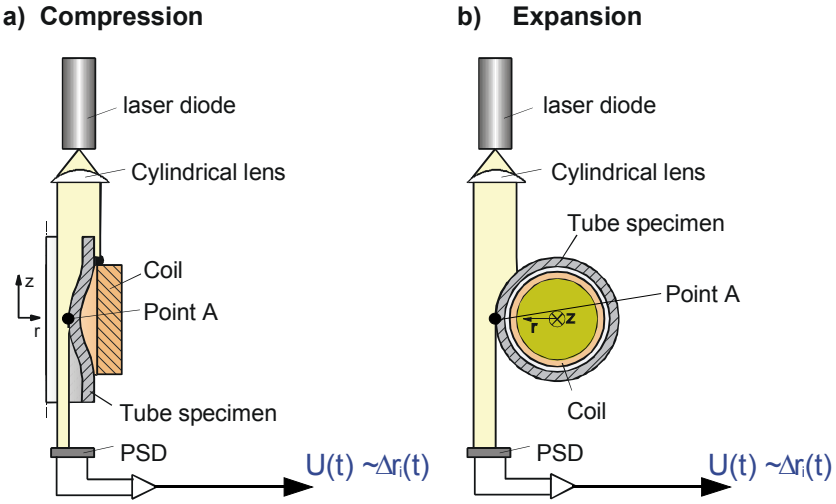

Figure 2: *On-line measurement system for radial displacement*

3 Finite Element Modelling

The finite element model consists of two different domains that are coupled in a staggered approach (see Figure 3).

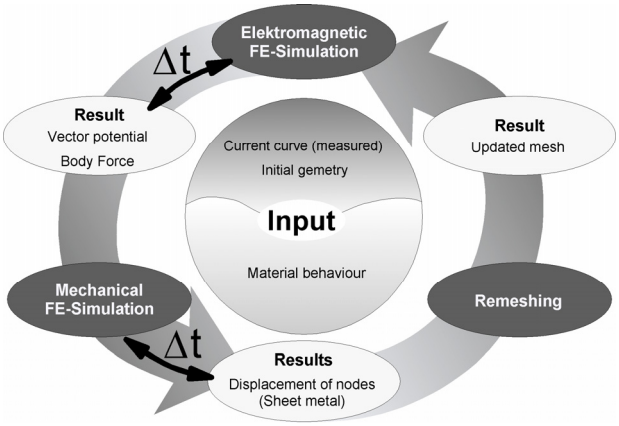

Figure 3: *Weak Coupling Procedure*

The mechanical sub-system allows the structure-dynamic simulation of the forming process. For this purpose the general-purpose-program MARC (version 2003) combined with user-subroutines is used. Contrary, the electromagnetic field simulation is done by a self developed FE-Code to determine the acting body forces inside the tube specimen.

The used weak coupling procedure is shown in Figure 3. Starting with an initial mesh in the electromagnetic domain, the body force distribution is calculated assuming a harmonic oscillating coil current with amplitude of 1kA. These force distribution is scaled with the measured coil current for a defined time interval Δt to ensure a transient evolution of acting forces during the mechanical analysis with Marc. The calculated deformation requires the update of the mesh for the surrounding air. Therefore a re-meshing algorithm is implemented based on a delauney triangulation to ensure the automated mesh generation during the coupled simulation. After finishing this, a new electromagnetic simulation will be carried out to update the body force distribution with respect to the actual geometry. In the following chapters the mentioned modules will be described.

3.1 Mechanical Model

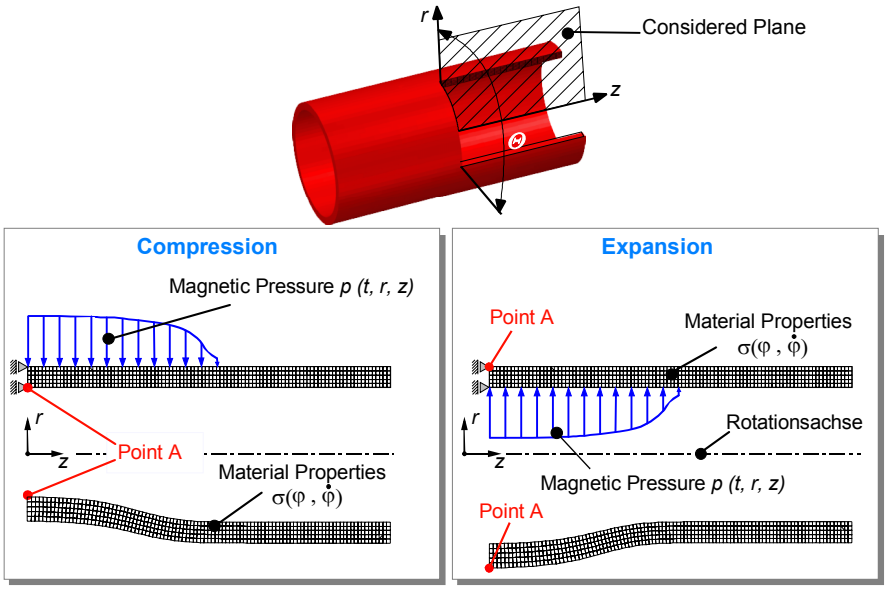

Figure 4: *Mechanical finite element model for tube compression and expansion*

The mechanical as well as the electromagnetic finite element model, makes use of the rotational symmetry of tool and work-piece. This simplification is possible, because the symmetrical pressure distribution causes a symmetrical deformation with very good concentricity of the sample even after the forming process. By utilising the symmetry of the tube, only half the geometry has to be considered. To ensure the consideration of inertia effects during the process an implicit time integration scheme (Newmark) has been applied to solve the equations of motion. The mechanical mesh was build up with approximately 400 iso-parametric four-node 2-½ D elements with bilinear shape function. Figure 4 shows the mesh of the modelled half with the applied load distribution depending from the chosen arrangement. The displayed load type (magnetic pressure as a surface load) is only for simplification because the body force is considered. The calculation of this load is done by a self-developed FE-Code, which is implemented via user-subroutines.

3.2 Electromagnetic Model

To simplify the time intensive transient calculation of the electromagnetic field, the following harmonic system will be solved.

$$([K] - \Omega \cdot [C]) \cdot (\{u_1\} + i \cdot \{u_2\}) = \{F_1 + i \cdot F_2\} \quad (1)$$

K:	Stiffness matrix	Ω:	Imposed circular frequency
C:	"Damping" matrix	A_e:	Magnetic vector potential
u_1, u_2:	Real and imaginary part of the DOF	ν_e:	time integrated electric scalar potential
F_1, F_2:	Real and imaginary part of the force	i:	Square root of -1

The vector potential A_e as well as the electric scalar potential ν_e are considered as a degree of freedom (DOF). This kind of modelling is necessary to ensure the capability of a massive conductor simulation with an appropriate current density calculation inside the windings. A detailed description of the implemented Matrices is given in [2].

Despite a typical number of 10,000 nodes, which are necessary to model the electromagnetic domain, short simulation times are required to reduce the over-all simulation time for the material determination. To ensure this, an iterative conjugate gradient sparse matrix solver is implemented to solve Equation (1). Beside the advantage of getting a fast solution, less memory storage is needed compared to conventional frontal solvers.

3.3 Re-meshing algorithm

Similar to the mentioned different simulation domains, two different finite element meshes are in usage. The first one is the mechanical mesh, shown in Figure 4. The element connectivity is unchanged over the whole calculation, but the nodal coordinates are changing because of the transient mechanical simulation.

The second mesh regards the electromagnetic field simulation. It has to be updated for each harmonic simulation. To reduce the time effort for the re-meshing procedure during the staggered simulation this area is subdivided into two parts: On the one hand a fixed mesh is used, which is unchanged during the whole simulation. This part includes the windings and the areas far away from the region where the deformation occurs. On the other hand, the region nearby the deformation area has to be re-meshed with respect to the tube contour. This is done automatically by a delauney triangulation.

4 Material behaviour and its description

The material behaviour is modelled as a function of plastic strain as well as from plastic strain rate. Despite the fact that EMF is nearly an adiabatic process, finite element simulations of the tube compression have shown a maximal temperature rise of approximately 20 K [3]. Therefore temperature effects on the yield stress are neglected.

With the aim using an optimisation algorithm for the automated modification of the material parameters, the mathematical description of the material must fulfil several demands. On the one hand the chosen parameters have to be suitable for modelling the material behaviour with respect to the physics and do not constrain it in an unrealistic

manner (e.g. by a insufficient number of parameters). On the other hand the number of parameters must be limited to apply an optimisation algorithm in a reasonable way with respect to the computational effort.

To overcome this conflict of aims a Bezier-Surface is used to approximate the flow curve array (see Figure 6). 16 control points are necessary to define the surface; each of them consists of 3 coordinates which over-all generates 48 independent parameters. By definition of reasonable restrictions (the quasi-static yield curve remains and upper boundaries for the strain and strain rate) the number of parameters can be reduced to 26.

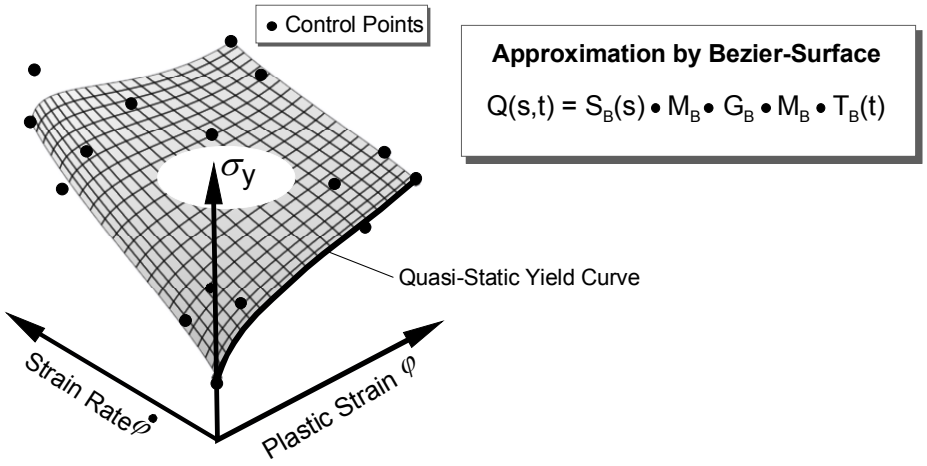

Figure 6: *Approximation of strain rate dependency via Bezier-Surface*

5 Optimisation algorithm

Searching for an optimum can be very time consuming. Especially, if it is completely unknown where the optimum is located. Independent from the used optimisation tool, it is necessary to define a point where the algorithm starts. In the present case, at least 26 parameters have to be defined with values, which are still unidentified. To overcome this problem, two optimisation strategies are applied. First, a physical based strategy will be used to determine starting parameters, which are located in the area of the optimum. These parameters are used by the second strategy to initialise the starting point and proceed with the optimisation process immediately.

5.1 Physical based optimisation

The basic idea of this pre-optimisation is the assumption of a constant amount of dissipated energy due to plastic deformation, independent from the hardening behaviour of the material. This assumption is not in accordance with the physical behaviour of the material, but it can be used as a rough estimation for the first optimisation stage.

The requirement for starting the optimisation is the knowledge about the quasi-static yield curve $\sigma_v(\varphi_v)$ of the tube specimen. During the forming process energy dissipates due to plastic deformation regarding Equation 2 (specific work is used for a simpler notification).

$$w = \int_0^{\varphi_v} \sigma_v \cdot d\varphi_v \tag{2}$$

A first simulation with the quasi-static yield curve is carried out and the radial displacement will be measured by the system described in chapter 2. The logarithmic tangential strain $\varphi_{33,\,\mathrm{exp}}$ is calculated from the on-line measurement using Equation 3 (Δr: radial displacement; r_0: initial radius). A scale factor f is defined by dividing the maximal tangential strain from the experiment by the one calculated during the finite element simulation (Equation 4).

$$\varphi_{33,\,\mathrm{exp}} = \ln\left(1 + \frac{\Delta r}{r_0}\right) \tag{3}$$

$$f = \frac{\max\left(\varphi_{33,\mathrm{exp}}\right)}{\max\left(\varphi_{33,\mathrm{sim}}\right)} \tag{4}$$

This factor is applied to the simulated equivalent plastic strain, which is considered as a function of time [$\varphi_v = f(t)$]. Remembering the basic assumption of this procedure regarding a constant amount of work independent from the hardening behaviour, it is obvious that an unbalanced system is generated (Equation 5 and 6).

$$w_{sim} \neq w_{sim,scale} \tag{5}$$

$$\int_0^{\varphi_v} \sigma_v \cdot d\varphi_v \neq \int_0^{\varphi_{v,scale}} \sigma_v \cdot d\varphi_{v,scale} \tag{6}$$

To get a balanced system, the yield stress has to be modified by a correction term $\Delta\sigma_v$ which can be seen as a function of the strain rate [$\Delta\sigma_v = f(\dot{\varphi}_v)$].

$$\int_0^{\varphi_v} \sigma_v \cdot d\varphi_v = \int_0^{\varphi_{v,scale}} \left(\sigma_v + \Delta\sigma_v\right) \cdot d\varphi_{v,scale} \tag{7}$$

Applying Equation 7 during the whole simulation procedure, the correction term $\Delta\sigma_v = f(\dot{\varphi}_v)$ can be determined for every increment directly. By updating the initially used quasi-static yield curve, the hardening behaviour becomes also a function from the strain rate $\sigma_v = f(\varphi_v, \dot{\varphi}_v)$. The described steps will be repeated until a) a rough agreement between simulation and experiment is achieved and b) the starting point of the subsequent optimisation strategy is well defined. In the present case 27 simulations has to be done to initialise the subsequent optimisation algorithm.

5.2 Numerical based optimisation

In the present case a “Downhill-Simplex” algorithm is used, which is not related to the simplex method of linear programming [4]. The method needs only function evaluations and requires no derivatives. Unfortunately it converges very slowly, because no information about a preferable direction like in a gradient-based optimisation strategy is given. But this disadvantage will be compensated by the algorithms robustness.

Using the simulation results from the previous optimisation stage, the initial simplex can be initialised with a suitable starting position and the optimisation can proceed. The function to be minimised is the deviation between simulated and measured radial displacement over the whole process time. If the obtained solution between two iterations remains static, the optimisation procedure will stop and the material description is found.

The described combination of the two strategies ensures a fast convergence for the determination of material parameters. A typical number of necessary iterations are about 120.

6 Determined material characteristic

Figure 7 shows the comparison between the measured and simulated tube narrowing (Figure 7a) and tube expanding (Figure 7b) by means of two different loading energies for each arrangement.

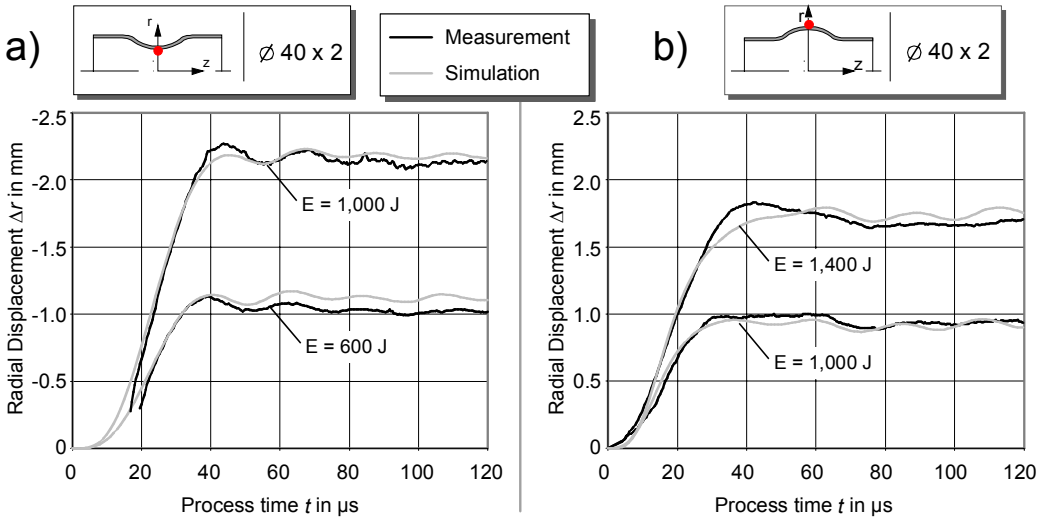

Figure 7: *Measured and simulated radial displacement*

Because of a measurement inaccuracy of approximately 0.1 mm an exclusive evaluation of the displacement deviations between the corresponding curves isn't meaningful. An additional check of the relevant eigenfrequencies is also advisable. Doing this, it can be seen that the simulation results are in good agreement with the experiment, except the tube expansion with a charging energy of 1,400 J. The experimental curve shows the typical "overshooting" of the displacement, followed by an untypical low frequent oscillation. This measured curve wasn't reached by any simulation result. A reason could be an insufficient roundness of the initial tube specimen. Spot tests have shown maximal deviations of about ± 0.2 mm. The influence of this has to be quantified by a 3-dimensional simulation with an accordant wall thickness distribution.

Figure 8 shows the corresponding yield curve array as a Bezier-Surface for the relevant strain and strain rate area for tube compression (Figure 8a) as well as for tube expansion (Figure 8b). Both yield curve arrays show a distinct hardening due to the achieved strain rate during the forming process, but the materials gets a higher strength in case of tube expansion. Reasons for this phenomenon could be the different hardening behaviour for tensile and compressive stressing, known from the literature as Bausch-

inger-effect. If this will become dominant for aluminium alloys to be formed with this process, the assumption of an isotropic material behaviour must be dropped. Instead of this, an initial anisotropy must be included and experiments for tube compression as well as for tube expansion has to be done for a complete material characterisation.

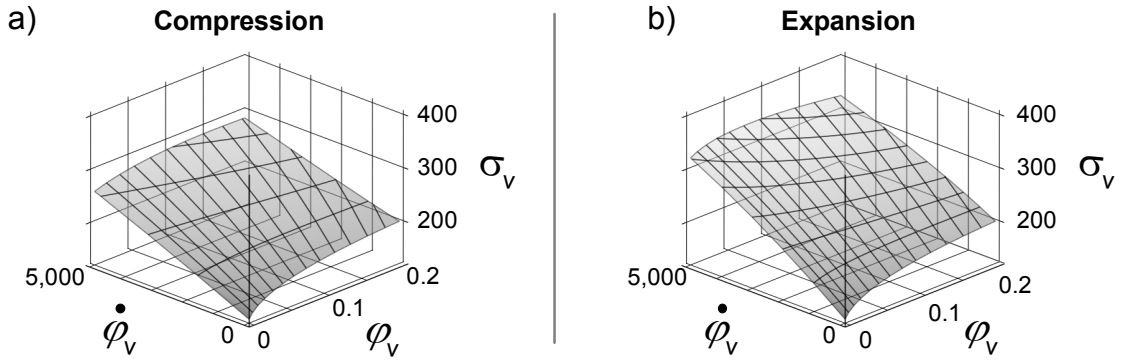

Figure 8: *Determined flow curve arrays*

7 Summary and Outlook

The present article describes the possibility to determine material characteristics by using the electromagnetic forming process for tube compression and tube expansion and an iterative weak coupled finite element simulation procedure. The experimental set-up is capable to achieve strain rates up to 10,000 s^{-1} where other techniques will start to fail. The simulation procedure allows a very fast simulation of the coupled field problem with a sufficient accuracy, which is essential for the determination of material parameters.

The presented results show a dependency on the direction of stressing. Therefore an initial anisotropic material behaviour inside the simulation has to be implemented and the effect on the determined material parameters has to be quantified. This approach is directly transferable to the material determination using the electromagnetic sheet metal forming process where effects of cinematic hardening can be expected.

References

[1] *Bauer, D.:* Der Einfluß hoher Formänderungsgeschwindigkeiten auf die Kaltumformung von Stahl Kupfer und Alumumium, Fortschrittberichte der VDI-Zeitschriften; Reihe 2, Nr. 26.

[2] SAS IP, Inc: Ansys Theory Reference, 11th edition, V5.6, 1999.

[3] *Brosius, A.; Kleiner, M.:* Ermittlung Gescgwindigkeitsabhängiger Fließkurven mittels Elektromagnetischer Umformung, Oral Presentation at 2. Kolloq. Elektromagnetische Umformung, 28. Mai 2003, Dortmund.

[4] *Nelder, J.A., and Mead, R.* 1965, Computer Journal, Vol. 7, pp. 308–313.